Improved mobility of AlGaN channel heterojunction material using an AlGaN/GaN composite buffer layer*

Wen Hui-Juan(温慧娟), Zhang Jin-Cheng(张进成)†, Lu Xiao-Li(陆小力), Wang Zhi-Zhe(王之哲), Ha Wei(哈 薇), Ge Sha-Sha(葛莎莎), Cao Rong-Tao(曹荣涛), and Hao Yue(郝 跃)

State Key Laboratory of Wide Band Gap Semiconductor Technology, School of Microelectronics, Xidian University, Xi'an 710071, *China*

(Received 12 August 2013; revised manuscript received 24 September 2013; published online 14 January 2014)

The quality of an AlGaN channel heterojunction on a sapphire substrate is massively improved by using an AlGaN/GaN composite buffer layer. We demonstrate an $Al_{0.4}Ga_{0.6}N/Al_{0.18}Ga_{0.82}N$ heterojunction with a state-of-the-art mobility of 815 $cm^2/(V\cdot s)$ and a sheet resistance of 890 $\Omega/\square$ under room temperature. The crystalline quality and the electrical properties of the AlGaN heterojunction material are analyzed by atomic force microscopy, high-resolution X-ray diffraction, and van der Pauw Hall and capacitance–voltage (C–V) measurements. The results indicate that the improved electrical properties should derive from the reduced surface roughness and low dislocation density.

Keywords: AlGaN channel, heterojunction, mobility, electrical properties

PACS: 73.40.Kp, 73.40.–c, 73.61.Ey, 78.30.Fs **DOI:** 10.1088/1674-1056/23/3/037302

1. Introduction

With the advantages of a wide band gap, high breakdown electric field strength, high electron saturation velocity, and so on, nitride-based semiconductors are promising for high-temperature, high-voltage, and high-frequency applications.[1–3] Since AlGaN (energy band gap $E_g = 3.4$ eV–6.2 eV) and AlN ($E_g = 6.2$ eV) have wider energy band gaps and higher breakdown field strength than GaN, AlGaN channel high electron mobility transistors (HEMTs) have been proved to hold higher breakdown voltages and better device stability than conventional GaN channel HEMTs.[4] Using AlGaN instead of GaN as the channel layer is one way to enhance the breakdown voltage and improve the output power. However, high-quality AlGaN material is hard to obtain. First, the large lattice mismatch results in a large number of dislocations; second, the stress generated when the islands merge will lead to cracks in the film; and third, the micro-particles produced by the pre-reaction fall in the growing surface will result in a large number of defects. This is why the materials reported in low-Al-composition $Al_xGa_{1-x}N$ channel HEMTs ($x = 0.16$ and $\mu = 645$ $cm^2/(V\cdot s)$,[5] $x = 0.2$ and $\mu = 259$ $cm^2/(V\cdot s)$,[6] $x = 0.15$ and $\mu = 505$ $cm^2/(V\cdot s)$,[7] $x = 0.06$ and $\mu = 590$ $cm^2/(V\cdot s)$[8]) have low mobility. This low mobility makes it hard to meet the requirements of the applications. To obtain better epitaxial quality and higher mobility, we used an AlGaN/GaN composition buffer layer and obtained an $Al_{0.4}Ga_{0.6}N/Al_{0.18}Ga_{0.82}N$ heterojunction with a state-of-the-art mobility of 815 $cm^2/(V\cdot s)$ and a sheet resistance of 890 $\Omega/\square$ at room temperature by metal organic chemical vapor deposition (MOCVD) on a sapphire substrate.

2. Experimental procedure

All the heterojunctions were grown using a low-pressure MOCVD system on two-inch c-plane sapphire substrates, and the schematic cross sections are shown in Fig. 1. Trimethylalumium (TMAl), triethylgallium (TEGa), and ammonia (NH_3) were used as the sources of Al, Ga, and N, respectively, and hydrogen was used as the carrier gas. Two kinds of AlGaN channel samples with different buffer layers were investigated, labeled samples A and B, respectively. The structures and growth conditions of the AlN nucleation layer, the AlGaN channel layer and the AlGaN barrier layer were the same for both samples. For sample A, the Al composition of the AlGaN buffer layer was fixed at 18%. For sample B, the AlGaN/GaN composite buffer layer was made of a 700 nm GaN and a 300 nm linearly graded[9] $Al_xGa_{1-x}N$ ($x = 0$–0.18) buffer layer, which was used to avoid the generation of a parasitic channel in the buffer layer. Following the growth of the buffer layer, a 600 nm $Al_{0.18}Ga_{0.82}N$ channel layer and a 22 nm $Al_{0.4}Ga_{0.6}N$ barrier layer were grown.

High-resolution X-ray diffraction (HRXRD) and atomic force microscopy (AFM) were used to evaluate the dislocation density and the surface morphology of the AlGaN film. The transport properties of the two samples were measured by van der Pauw Hall measurements from 77 K to 573 K. Capacitance voltage (C–V) analysis was performed at 100 kHz using a mercury-probe contact.

*Project supported by the National Science and Technology Major Project of the Ministry of Science and Technology of China (Grant Nos. 2011ZX01002-002 and 2013ZX02308-002), the Fundamental Research Funds for the Central Universities of Ministry of Education of China, and the National Natural Science Foundation of China (Grant Nos. 61204006 and 61106063).

†Corresponding author. E-mail: jchzhang@xidian.edu.cn

© 2014 Chinese Physical Society and IOP Publishing Ltd

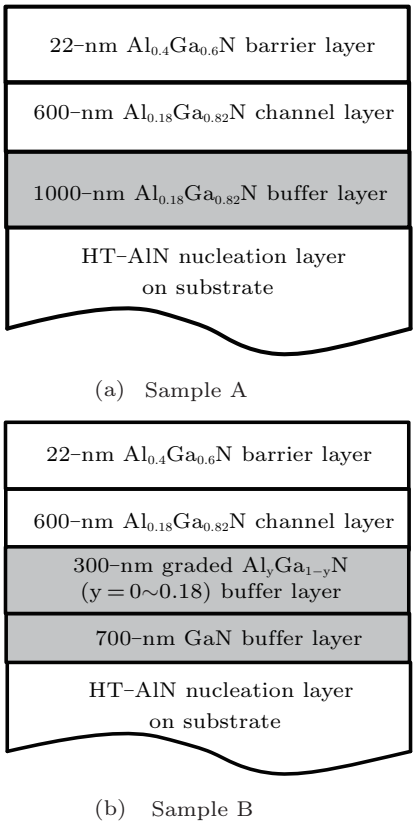


Fig. 1. Schematic cross sections of samples A (a) and B (b).

3. Results and discussion

Figure 2 shows the energy band diagrams of the two samples simulated by solving the one-dimensional (1D) Poisson equation. The two samples have the same energy band diagram, which means that they have the same carrier confinement. Because the aggregate thickness of the lower AlGaN layers both exceed 600 nm, the channel layers of the two samples are both relaxation, and the stress of the interface between the barrier layer and the channel layer is the same. The polarization is also the same, so we mainly consider the influence of the composition buffer layer.

The HRXRD and AFM results of the two samples are presented in Table 1. Typical AFM images with a 3 μm×3 μm scan area of the surfaces of the two samples are shown in Fig. 3. Many V-pits are generated by dislocations and almost no obvious atom steps can be seen in sample A. In sample B, fine atomic steps can be clearly seen with few small V-pits. The V-pit density of sample A is 1.06×10^{10} cm^{-2}, which is about 3.3 times larger than that of sample B (3.2×10^{9} cm^{-2}). The root mean square (RMS) roughness and the surface *P*–*V* height of sample B are 0.190 nm and 2.418 nm, which are lower than those of sample A (0.307 nm, 3.065 nm). The results indicate that the composite buffer layer can improve the quality of the AlGaN material.[10]

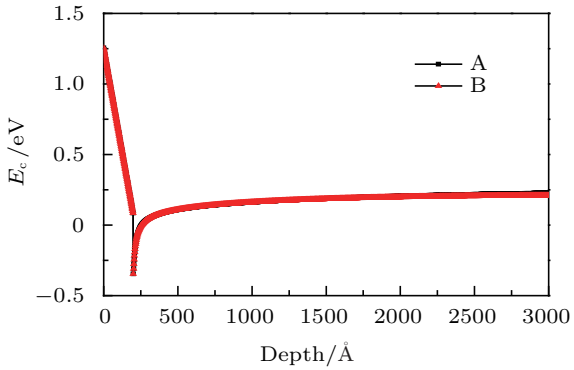


Fig. 2. (color online) Energy band (E_c) diagram of samples A and B.

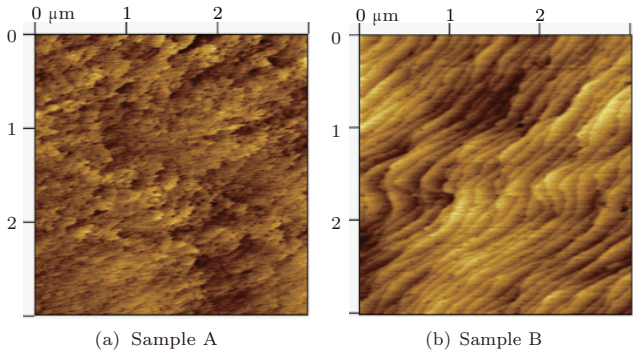


Fig. 3. (color online) The 3 μm×3 μm AFM images of samples A (a) and B (b).

Table 1. Summary of the AFM and HRXRD measurements for samples A and B.

	RMS/nm	*P*–*V* height/nm	(0002) FWHM /arcsec	(10-12) FWHM /arcsec	Threading dislocation density/cm^{-2}	Edge dislocation density/cm^{-2}	Pit density /cm^{-2}
sample A	0.307	3.065	324.8	2041.9	2.12×10^{8}	2.4×10^{10}	1.06×10^{10}
sample B	0.190	2.418	241.1	928.7	1.17×10^{8}	4.6×10^{9}	3.20×10^{9}

Figure 4(a) shows the (0002) XRD 2θ–ω scans of samples A and B. A peak signal around 34.7°, originating from the AlGaN channel layer, a peak signal around 35.1°, originating from the AlGaN barrier layer, and a peak signal around 36.0°, originating from the AlN nucleation layer, were observed in samples A and B, respectively. Additionally, a peak signal around 34.5°, originating from GaN, was observed in sample B. In particular, the peak signals originating from the AlN nucleation layer, GaN buffer layer, AlGaN buffer layer, AlGaN channel layer and AlGaN barrier layer were observed clearly in sample B. This indicates that the grown AlGaN-channel heterojunction has good crystalline quality.

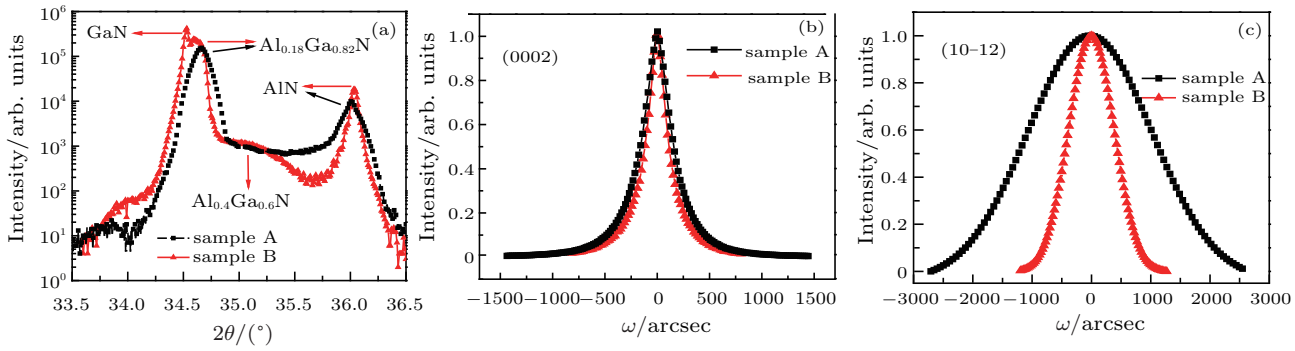


Fig. 4. (color online) The (a) (0002) ω–2θ scan, (b) (0002) rocking curves, and (c) (10-12) rocking curves for samples A and B.

In order to further evaluate the crystalline quality, the X-ray rocking curves for the (0002) and (10-12) diffractions of the channel layers were measured by HRXRD. Figures 4(b) and 4(c) clearly show the (0002) and (10-12) ω-scan rocking curves, which were obtained through the normalized angle and intensity in order to contrast and determine the full widths at half maximum (FWHMs) of the rocking curves. The (0002) and (10-12) FWHMs of sample A are 324.8 arcsec and 2041.9 arcsec, respectively, and the (0002) and (10-12) FWHMs of sample B are 241.1 arcsec and 928.7 arcsec, respectively, which are obviously smaller than those of sample A. The pit density from the AFM measurements also shows the same result. It is believed that threading dislocation affects the FWHMs of the rocking curves for the (0002) peak, and edge dislocation affects those for the (10-12) peak.[11] The dislocation density can be calculated with $D_{\mathrm{B}} = \beta^2/4.36b^2$, where D_{B} is the dislocation density, β is the ω-FWHM, and b is the length of the Burgers vector. The specific values of the dislocation densities are shown in Table 1. It is observed that the gap in the threading dislocation densities in samples A and B is small, but the edge dislocation density of sample B is decreased greatly by employing a composite buffer layer.

The reduction in RMS roughness and the improvement in the material quality are also attributed to the application of an AlGaN/GaN composite buffer layer. In particular, the crystalline quality and surface morphology of the materials are related to the adatom diffusion on the growing surface.[12] Compared with Ga adatoms, Al adatoms are easily "trapped" at sites that do not correspond to the ideal lattice positions due to the low adatom diffusion, resulting in the difficulty of obtaining a high quality and uniform AlGaN epitaxial layer. In contrast, the Ga adatoms are highly mobile and the step-flow growth mode of GaN results in a flat surface. It is observed that as the thickness increases, the crystalline quality of the GaN epitaxial layer is improved with a flat surface due to parts of the dislocations annihilating and merging along the growth direction, but the quality improves slowly when the thickness exceeds 600 nm.[13] Owing to the small lattice mismatch, a 300 nm high-quality linearly graded $\mathrm{Al}_x\mathrm{Ga}_{1-x}\mathrm{N}$ ($x = 0$–0.18) buffer layer can be relatively easily grown on a 700 nm high-quality GaN buffer layer.

Figure 5(a) shows the carrier concentration distribution of the two samples, which is obtained by associating

$$N_{\mathrm{D}} = \frac{-2}{q\varepsilon A^2[\mathrm{d}(1/C^2)/(\mathrm{d}V)]},$$

$W = A\varepsilon/C$, and using the measured C–V values, where N_{D} is the impurity concentration of the n region, $V(x)$ is the potential of the space charge region x, q is the electron charge, W is the depth of the barrier region, and ε is the dielectric constant.[14]

The results show that on one hand, no parasitic channel is formed in the interface of the AlGaN/GaN composite buffer layer due to the insertion of a graded $\mathrm{Al}_x\mathrm{Ga}_{1-x}\mathrm{N}$ layer between the $\mathrm{Al}_{0.18}\mathrm{Ga}_{0.82}\mathrm{N}$ channel layer and the GaN buffer layer, and on the other hand, the background carrier concentration is lower, which indicates that few residual carriers exist in the buffer layer. Therefore, these kinds of AlGaN channel HEMTs will have better off-state characteristics.[15]

Figure 5(b) shows the transport properties of the two-dimensional electron gas (2DEG) in both samples. It is clear that electron mobility is greatly improved from low temperature to high temperature by using a composite buffer layer. It has been reported that low-temperature mobility is limited by alloy disorder scattering, interface roughness scattering, and dislocation scattering mechanisms.[16–19] In our case, the mobility of sample B at 77 K is 1080 $\mathrm{cm}^2/(\mathrm{V{\cdot}s)}$, which is larger than that of sample A (467 $\mathrm{cm}^2/(\mathrm{V{\cdot}s)}$), and the considerably improved mobility can be attributed to lower dislocation density and better interface roughness. The mobility of sample B at 300 K is 815 $\mathrm{cm}^2/(\mathrm{V{\cdot}s)}$, while the mobility of sample A at 300 K is 281 $\mathrm{cm}^2/(\mathrm{V{\cdot}s)}$. At high temperature, the mobility of sample B is 200 $\mathrm{cm}^2/(\mathrm{V{\cdot}s)}$, which is about two times larger than that of sample A (113 $\mathrm{cm}^2/(\mathrm{V{\cdot}s)}$). The difference in the mobility between samples A and B becomes smaller and smaller with the increase in temperature, owing to many scattering mechanisms (longitudinal optical phonon scattering, acoustic phonon scattering, Piezoelectric field scattering, interface roughness scattering, and alloy disorder scattering) affecting the mobility to a certain extent from 200 K to 400 K.[18] At high temperature, the main scattering mecha-

nism is optical phonon scattering.[18] In particular, the mobility of sample B at 573 K is 200 $cm^2/(V\cdot s)$, almost the same as the value of 210 $cm^2/(V\cdot s)$ in the GaN channel heterostructure reported by Wang *et al*.[20] The sheet density of the AlGaN channel material changes little with temperature. These results indicate that the electrical properties of the AlGaN channel material degrade relatively slowly at high temperature. This is appropriate for high-temperature and high-voltage applications.

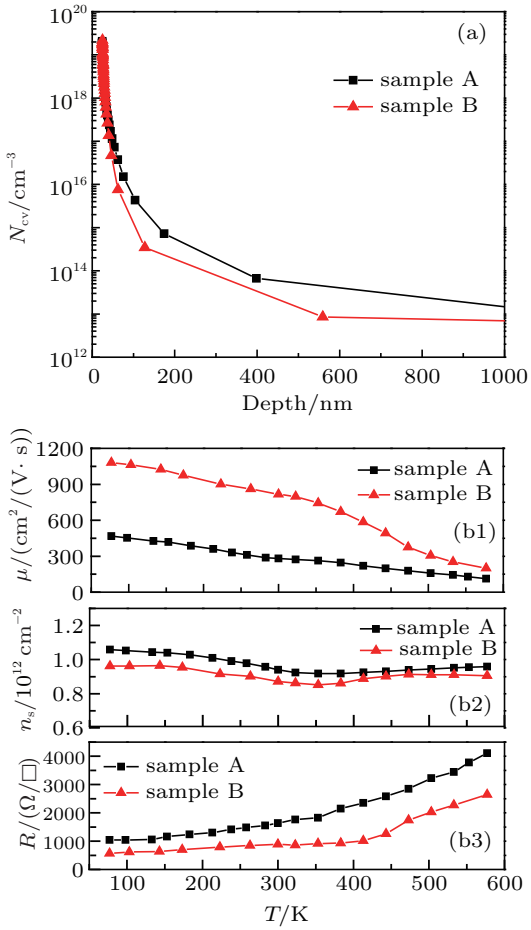


Fig. 5. (color online) The depth profile of the carrier concentration extracted from the *C*–*V* curve (a), and the temperature dependence of the Hall electron mobility μ (b1), sheet carrier density n_s (b2), and sheet resistance R (b3) of samples A and B.

The mobility was improved greatly and the resistance rapidly decreased using the AlGaN/GaN composition buffer layer. To our knowledge, the Hall mobility of sample B is 815 $cm^2/(V\cdot s)$, which is the best result so far, owing to the reduced interface roughness scattering and the lower dislocation density. However, the mobility of sample B is still much lower than the conventional AlGaN/GaN heterojunction, and the sheet resistances of the two samples are larger than those of the GaN channel HEMTs due to alloy disorder scattering in the AlGaN channel layers.[9] To further reduce the sheet resistance of the AlGaN channel HEMTs, it is necessary to further reduce the dislocation density and improve the crystalline quality of the AlGaN channel layer. The existence of disordered distribution of Ga atoms and Al atoms induces alloy disorder scattering at the interface between the AlGaN channel layer and the barrier layer. Therefore, we can insert an AlN interlayer between the AlGaN channel layer and the barrier layer, and alloy disorder scattering from the barrier may be reduced, as reported in the AlGaN/GaN heterojunction.[21] As for sample B, if an AlN interlayer was inserted not only between the AlGaN channel layer and barrier layer but also between the AlGaN channel layer and the buffer layer, an increment of 2DEG mobility will be observed.

4. Conclusion

In conclusion, an AlGaN channel heterojunction with a state-of-the-art electron mobility[5–8] of 815 $cm^2/(V\cdot s)$ and a sheet resistance of 890 Ω/□ at room temperature was obtained by using an AlGaN/GaN composite buffer layer. It is observed that the use of an AlGaN/GaN composite buffer layer can reduce surface roughness scattering and alloy disorder scattering, thus improving material quality. The improvement in the crystalline quality of the AlGaN channel heterojunction is essential to improving the mobility and reducing the sheet resistance of 2DEG, which is beneficial in improving the electrical properties.

References

[1] Ambacher O 1998 *J. Phys. D: Appl. Phys.* **31** 2653
[2] Zhang K, Cao M Y, Lei X Y and Hao Y 2013 *Chin. Phys. B* **22** 097303
[3] Mishra U K, Shen L, Kazior T E and Wu Y F 2008 *Proc. IEEE* **96** 287
[4] Nanjo T, Takeuchi M, Suita M, Oishi T, Abe Y, Tokuda Y and Aoyagi Y 2008 *Appl. Phys. Lett.* **92** 263502
[5] Nanjo T, Takeuchi M, Imai A, Oishi T, Abe Y and Yagyu E 2009 *Electron. Lett.* **45** 1346
[6] Hashimoto S, Akita K, Yamamoto Y, Ueno M, Nakamura T, Yafune N and Amano H 2012 *Phys. Status Solidi* **9** 373
[7] Nanjo T, Suita M, Oishi T, Abe Y, Yagyu E, Yoshiara K and Tokuda Y 2009 *Electron. Lett.* **45** 424
[8] Raman A, Dasgupta S, Rajan S, Speck J S and Mishra U K 2008 *Jpn. J. Appl. Phys.* **47** 3359
[9] Raghavan S and Redwing J 2005 *J. Appl. Phys.* **98** 023515
[10] Meng F N, Zhang J C, Zhou H, Ma J C and Xue J S 2012 *J. Appl. Phys.* **112** 023707
[11] Moram M A and Vickers M E 2009 *Rep. Prog. Phys.* **72** 036502
[12] Zywietz T, Neugebauer J and Scheffler M 1998 *Appl. Phys. Lett.* **73** 487
[13] Lebedev V, Tonisch K, Niebelschütz F, Cimalla V, Cengher D, Cimalla I, Mauder C, Hauguth S, Ambacher O, Morales F M, Lozano J G and González D 2007 *J. Appl. Phys.* **101** 054906
[14] Ni J Y, Zhang J C, Hao Y, Yang Y, Chen H F and Gao Z Y 2007 *Acta Phys. Sin.* **56** 6629 (in Chinese)
[15] Nanjo T, Takeuchi M, Imai A, Suita M, Oishi T, Abe Y, Yagyu E, Kurata T, Tokuda Y and Aoyagi Y 2009 *Electron. Lett.* **45** 1346
[16] Zanato D, Gokden S, Balkan N, Ridley B K and Schaff W J 2004 *Semicond. Sci. Technol.* **19** 427
[17] Asgari A, Babanejad S and Faraone L 2011 *J. Appl. Phys.* **110** 113713
[18] Lisesivdin S B, Acar S, Kasap M, Ozcelik S, Gokden S and Ozbay E 2007 *Semicond. Sci. Technol.* **22** 543
[19] Wang J X, Yang S Y, Wang J and Wang Z G 2013 *Chin. Phys. B* **22** 077305
[20] Wang M J, Shen B, Xu F J, Wang Y, Xu J, Huang S and Zhang G Y 2007 *Appl. Phys. A* **88** 715
[21] Elhamri S, Mitchel W C, Mitchell W D, Landis G R, Berney R and Saxler A 2007 *Appl. Phys. Lett.* **90** 042112